Twinning induced nanostructure formation during cryo-deformation

2014 IOP Conf. Ser.: Mater. Sci. Eng. 63 012157

(http://iopscience.iop.org/1757-899X/63/1/012157)

Twinning induced nanostructure formation during cryo-deformation

M Klimova[1], G Dyakonov[2], S Zherebtsov[1], G Salishchev[1] and D Molodov[3]
[1] Belgorod State University, Pobeda 85, Belgorod 308015, Russia
[2] Ufa State Aviation Technical University, K.Marks 12, Ufa 450000, Russia
[3] Institute of Physical Metallurgy and Metal Physics, RWTH Aachen University, D-52056 Aachen, Germany

E-mail: klimova_mv@bsu.edu.ru

Abstract. In the present work the influence of cryo-rolling to a true strain ε=2.66 on twinning and formation of ultrafine-grained/nanostructure in commercial-purity titanium and Fe-0.3C-23Mn-1.5Al TWIP steel was quantified using scanning and transmission electron microscopy. Different influence of twinning on the kinetics of microstructure refinement and nanostructure formation in titanium and steel was revealed. In titanium twin boundaries during deformation transform into arbitrary high-angle grain boundaries thereby promoting the microstructure refinement to a grain/subgrain size of 80 nm. In steel twinning has less pronounced influence on the microstructure refinement. However, very fine grains/subgrains with the size of 30-50 nm was observed in the microstructure after rolling at 77K to a true thickness strain of 2.66.

1. Introduction

According to the well-known definition [1] any SPD process is associated with a very high straining of a material via various deformation methods. Correspondingly the main attention of researchers is focused both on the way to attain a high level of strain and on the microstructure of severely deformed metallic materials.

Meanwhile the grain microstructure of some metals and alloys refines quite readily even after relatively small strain. For example acicular microstructure of two-phase titanium alloys with a dense network of interphase boundaries transforms into an uniform globular ultrafine microstructure with a grain size of 0.3 μm already after 70% of height reduction at 550°C [2]. Furthermore, in the hexagonal close packed (HCP) metals and some steels with low stacking-fault energy (SFE) a prompt microstructure refinement occurs by twinning due to a formation of a large number of high-angle boundaries in the very beginning of deformation [e.g. 3, 4]. Therefore, twinning can be considered as a tool promoting formation of ultrafine-grained or nanostructure at a relatively small strain by utilizing the conventional metal-forming methods. Indeed, the microstructure with a grain size between 100 and 200 nm could be obtained via sheet rolling at room temperature to a true strain of $\varepsilon \approx 2.66$ [3].

Low deformation temperature increases the critical resolve shear stress of slip while almost does not change that of twinning [5] thereby intensifying considerably the contribution of twinning in microstructure evolution at cryogenic temperatures. This in turn should affect the kinetics of the microstructure refinement during further deformation (after ceasing of twinning). Indeed, some previous investigations [6, 7] have shown a potentiality of the microstructure refinement to the nanoscale after cryo-deformation of commercial-purity (CP) Ti. However, the microstructure evolution during large cryo-deformation of metals and alloys which deform by twinning has still been investigated only poorly. Furthermore, it is of interest to check whether a similar approach can be applied for the nanostructure formation in other materials with efficiently operating deformation twinning as, for example, TWIP steels. Therefore, the aim of the present work was to quantify the influence of cryo-rolling on the microstructure evolution and nanostructure formation during large deformation of CP titanium and Fe-0.3C-23Mn-1.5Al TWIP steel.

2. Material and Procedures

A 4 mm thick slab of CP titanium (Ti-balance; impurities in wt.% less than: 0.2 Fe, 0.1 Si, 0.07 C, 0.04 N, 0.12 O) and 10 mm thick slab of Fe-0.3C-23Mn-1.5Al TWIP steel were used in the present investigation. In the as-received condition, the microstructure of the program materials consisted of equiaxed grains with an average size of 15 μm (CP Ti) or 40 μm (steel). The grains in each material contained few twins and essentially no internal substructure.

Samples with dimensions of 4 mm ×10 mm × 30 mm were rolled unidirectionally in few passes at liquid nitrogen temperature (77K) using a fixed rolling speed of 30 mm/s to a total true strain of 2.66 (thickness strain of 93%). Prior to cryo-rolling, each preform was encapsulated between sacrificial either titanium (for Ti specimen) or steel (for steel specimen) sheets which were joined by spot welding. The pack was then cooled to 77K in liquid nitrogen and rolled between room-temperature rolls. The temperature of the canned workpiece during such a pack-rolling process did not increase by more than 20°. To ensure nearly isothermal deformation, each pack was cooled in liquid nitrogen between each rolling pass.

The microstructure in the mid-layer of the sheet specimens was characterized by means of transmission electron microscopy (TEM) using a JEOL JEM-2100FX transmission electron microscope and electron-backscatter-diffraction (EBSD) utilizing a Quanta 600 scanning-electron microscope (SEM). The border between low-angle boundaries (LABs) and high-angle boundaries (HABs) was assumed to be 15°. Grain misorientations below 2° were excluded from the data analysis.

To determine the post-rolling mechanical properties, tension tests were conducted at room temperature. For this purpose, flat specimens with gauge dimensions of 16 mm length × 3 mm width × 1.5 mm (or 0.3mm in case of the sheet rolled to ε=2.66) thickness were machined and pulled at a constant crosshead speed of 1 mm/min in a screw-driven test machine to fracture.

3. Results

3.1 Microstructure evolution in Ti

Transmission electron microscopy of ε = 0.1 rolled specimens of Ti reveals clusters of twins of various widths (figure 1a). According to EBSD data the observed twins belong mainly to $(11\bar{2}2)$ (twin/matrix misorientation angle of 64.62° around a common $<10\bar{1}0>$ axis), and $(11\bar{2}3)$ (86.98° around $<10\bar{1}0>$) families. The average twin thickness is 1.2 μm (figure 2b). Dislocation density in different parts of the microstructure varies in a wide interval: from separate dislocations to dense pile-ups. An increase in strain up to ε = 0.35 (figure 1b) results in an increase of the twin number, whereas their thickness decreases to 0.7 μm (figure 2b). Twin crossing and secondary twinning slices the microstructure into rectangular fragments with the size of 0.4 μm. At $\varepsilon \geq 0.51$ the formation of new twins is no longer observed; in turn, the cease of twinning results in a pronounced increase of the dislocation density (figure 2a). Substructure consists of dislocation boundaries formed in regions between twins (figure 1c). Twins are divided into parts with different contrast.

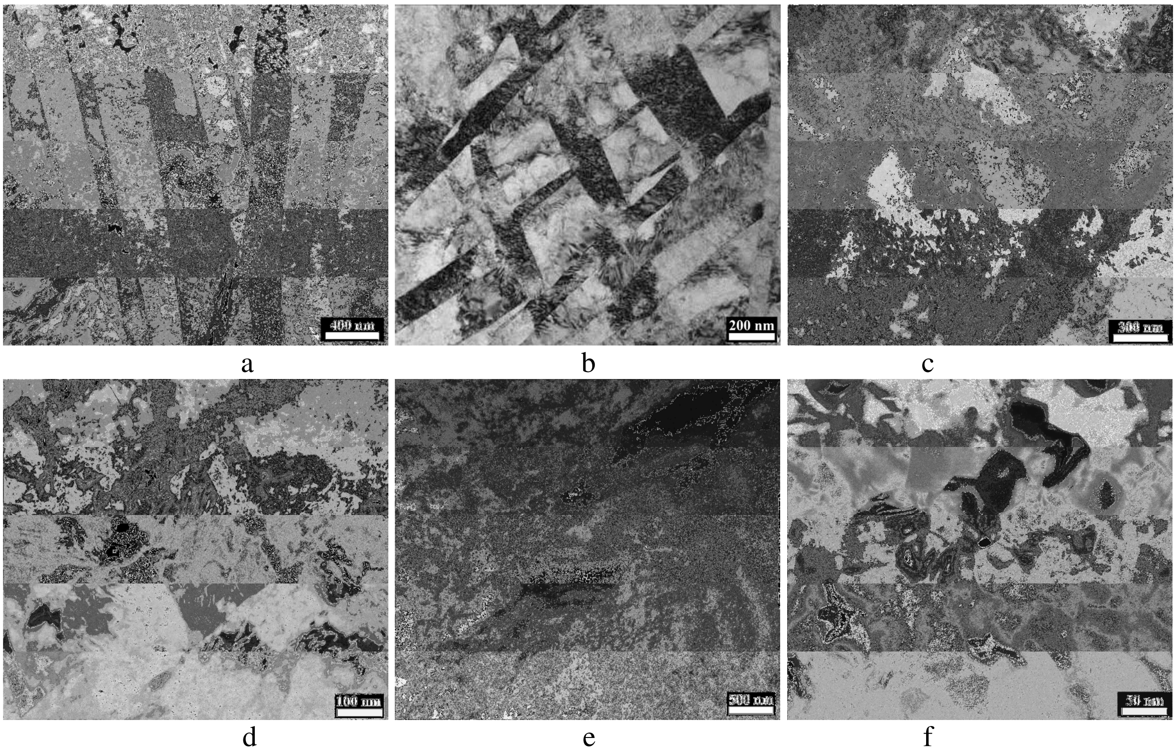

Figure 1. Transmission-electron micrographs of CP Ti rolled at 77K to a true strain ε of a) 0.1; b) 0.35; c) 0.51; d, e) 0.92; f) 2.66.

Cryo-rolling of Ti up to ε = 0.92 results in a formation of (sub)grains either due to dividing of twins by transversal boundaries or via formation of deformation-induced high-angle boundaries from dislocation walls and subgrains (figure 1d). Finally a heterogeneous microstructure forms consisting of grains/subgrains of various sizes (from 50 to 500 nm) and remains of twins (figure 1e). An increase in strain up to ε = 2.66 enhances the microstructure homogeneity and decreases grain size. The average grain/subgrain size was found to be 80 nm (figure 1f). The presence of equiaxed and dislocation free (sub)grains with thin smooth boundaries (figure 1f) suggests the development of recovery and even recrystallization processes that seems to be quite unusual for such a low temperature. However, high stresses can in some cases compensate for the insufficient thermal activation and induce local migration of grain boundaries and recrystallization [8-10].

Dislocation density measurements show three stages of its increase in both the matrix and the twins of cryo-rolled material (figure 2a). The first stage, characterized by a moderate rate of the increase in dislocation density, is observed in the range of ε from 0 to 0.35. During the second stage (for strains between ~0.35 and 0.55), the dislocation density increases very rapidly. The third stage is associated with the virtually steady-state dislocation density. The dislocation density in the twins is slightly higher than that in the matrix at the initial stages of deformation (ε ≤ 0.3), and then the difference disappeared (figure 2a). A rather low dislocation activity in the beginning of a deformation suggests that the early plastic deformation at 77K is accommodated by twinning rather than by slip. Such a trend may perhaps be ascribed to the increase in the critical resolved shear stress for slip with decreasing deformation temperature [11].

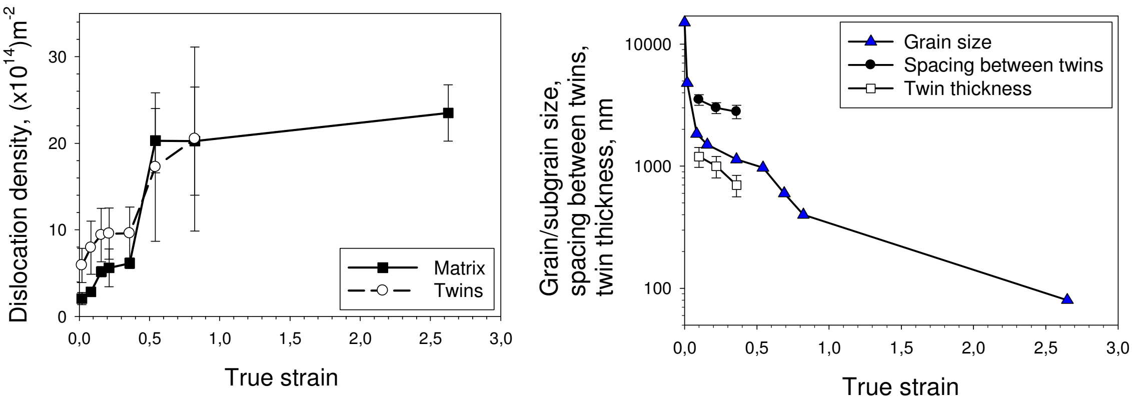

Figure 2. Dislocation density in the investigated Ti samples as a function of strain (a) and grain/subgrain size, twin thickness and spacing between twins as a function of true strain. Data for grain size in (b) were obtained by means of EBSD analysis (in the interval of ε_h = 0 - 0.92) and TEM (ε = 2.66).

Further quantitative insight into the microstructure evolution was obtained from EBSD measurements of the average grain size following rolling to various strain levels ($\varepsilon_t \leq 0.92$) (figure 2b); the EBSD measurements were supplemented by TEM observations for the largest strain (i.e., ε = 2.66). The grain size decreases very quickly with strain for $\varepsilon \leq 0.2$. This behavior is obviously associated with the twinning that is apparent from the evolution of twin thickness and spacing between twins (figure 2b). In the interval of strain between 0.2 and 0.35, the decrease in grain size becomes slower, most likely due to the exhaustion of twinning. During further rolling the grain size continued to decrease attaining after ε = 2.66 a grain/subgrain size of ~80 nm.

3.2 Microstructure evolution in Fe-0.3C-23Mn-1.5Al steel

According to SEM and TEM analysis, twinning in steel during cryo-rolling onsets at $\varepsilon \approx 0.05$ (at room temperature the onset of twinning is observed at $\varepsilon \approx 0.1$). The initial grains become divided by parallel or crossing twins into rather small pieces of various shapes ans sizes (figure 3a). All examined twins belong to the family (111) <112> (twin/matrix misorientation of 60° around a <111> axis). The minimum thickness of twins in the beginning of deformation was found to be ~ 10 nm; however, much thicker twins up to 300 nm are also observed. The matrix practically does not contain substructure or dislocation pile-ups at this stage of deformation (figure 4a). With increase in strain parallel twins cluster into bands; the number of twins within a band usually does not exceed 10 (figure 3b). The average thickness of newly-formed twins slightly decreases with strain (figure 4b). In some thick twins (100-500 nm) secondary twins form.

The dislocation density increases in the matrix relatively fast at the initial stages of stain however after ε = 0.2 the increase in the dislocation density becomes much slower (figure 4a). Deformation above ε = 0.2 give rise to a cellular microstructure with a high dislocation density (figure 3c and 4a). One of features of the largely strained microstructure of Fe-0.3C-23Mn-1.5Al steel is associated with the almost complete disappearing of twin boundaries (figure 3d,e). Obviously, this is an only seeming effect most likely associated with rotation of the twin planes towards the rolling plane, fragmentation of twins and decoration ot twin boundaries by high density dislocation arrays. At the same time, in contrast to Ti, formation of new extensive deformation-induced boundaries was almost not observed during large deformation. The steel microstructure after ε = 2.66 at low magnification can be described as a cellular one with the size of cells of 200 – 400 nm. At higher magnifications the microstructure consists of irregular dislocation pile-ups of different shapes and sizes and very small grains with the size of ~30-60 nm surrounded by high-angle boundaries (figure 3d,e).

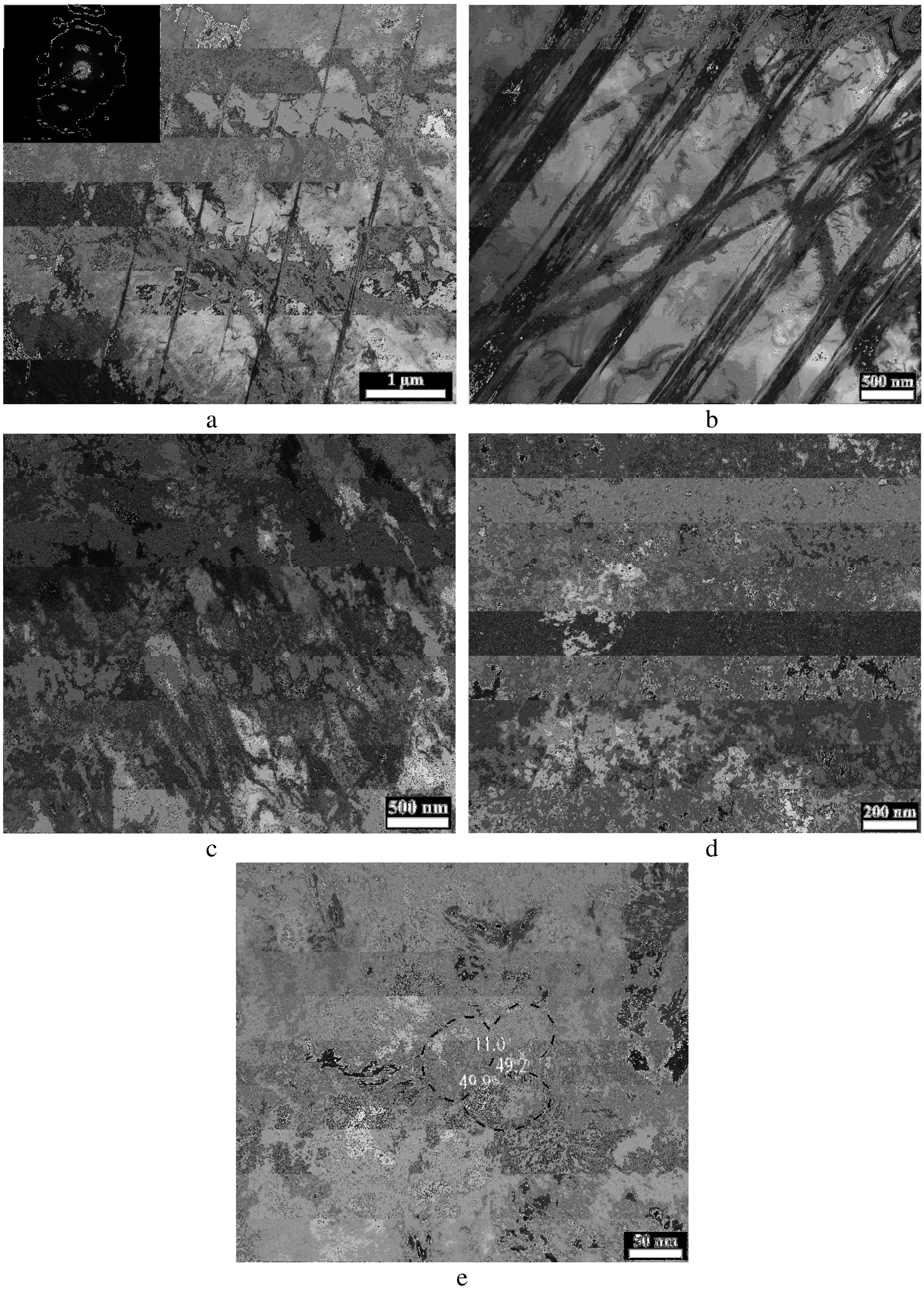

Figure 3. Transmission-electron micrographs of Fe-0.3C-23Mn-1.5Al steel rolled at 77K to a true strain ε of a) 0.05 (a); 0.1 (b); 2.66 (c-e). Diffraction patterns (inserts in 3a) obtained for the zone axis [110] shows the presence of twin reflexes.

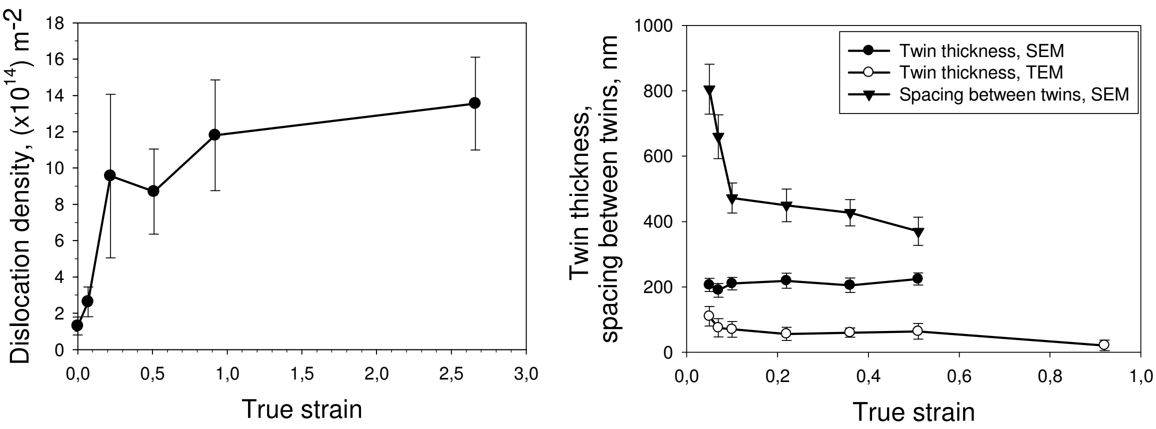

Figure 4. Dislocation density in Fe-0.3C-23Mn-1.5Al steel samples as a function of strain (a) and twin thickness and spacing between twins as a function of true strain. Data for twin thickness in (b) were obtained by means of SEM and TEM analysis.

A comparative analysis of the microstructure evolution (figure 3), changes of the dislocation density and parameters of twinning (twin thickness and spacing between twins) (figure 4) reveals that microstructure of the TWIP steel during cryo-deformation evolves distinctly different in comparison with titanium. It seems that in the steel twinning and dislocation slip does not compete between each other but rather develop simultaneously. In the interval of strain of $\varepsilon = 0$ - 0.2 a decrease of the spacing between twins (which is associated with an increase of the number of twins) is accompanied by the fast increase in the dislocation density. At ε between 0.1 and 0.2 the twinning generally ceases and the further microstructure evolution is associated with the development of the cellular microstructure. The formation of new individual grains surrounded by deformation-induced high-angle boundaries are observed only at very high strains.

3.3 Mechanical behavior of Ti and Fe-0.3C-23Mn-1.5Al steel

Typical true stress - true strain curves derived from load-stroke data prior to necking for tension testing of samples previously rolled at 77K to various strains are shown in figure 5. For the both examined materials, the samples rolled to $\varepsilon \leq 0.36$ exhibited a steady increase in the true stress with strain and a relatively high uniform elongation of ~0.05-0.11 in case of Ti and ~0.1-0.55 in case of Fe-0.3C-23Mn-1.5Al steel. An increase of ε during cryo-rolling up to 0.51 - 2.66 essentially resulted in the elimination of the strain hardening stage and early necking, which is typical for severely cold-worked materials.

Principal differences in the mechanical behavior of investigated titanium and steel comprised the lower flow stress, strain-hardening rate, and ductility obtained for Ti samples. However, heavily rolled titanium and steel had somewhat similar mechanical behavior during tension except for the substantially higher absolute strength of the steel.

From an application standpoint it is worth noting that the maximum ultimate tensile strength of Ti after cryo-rolling is ~1100 MPa, which is very close to the respective values of titanium alloys such as Ti-6Al-4V. In case of Fe-0.3C-23Mn-1.5Al steel the maximum ultimate tensile strength is ~1800 MPa. However, most interesting combination of properties is demonstrated by the 20% cryo-rolled steel, which shows yield stress of about 680 MPa, ultimate tensile strength of 1230 MPa and uniform elongation more than 30% (Figure 5b).

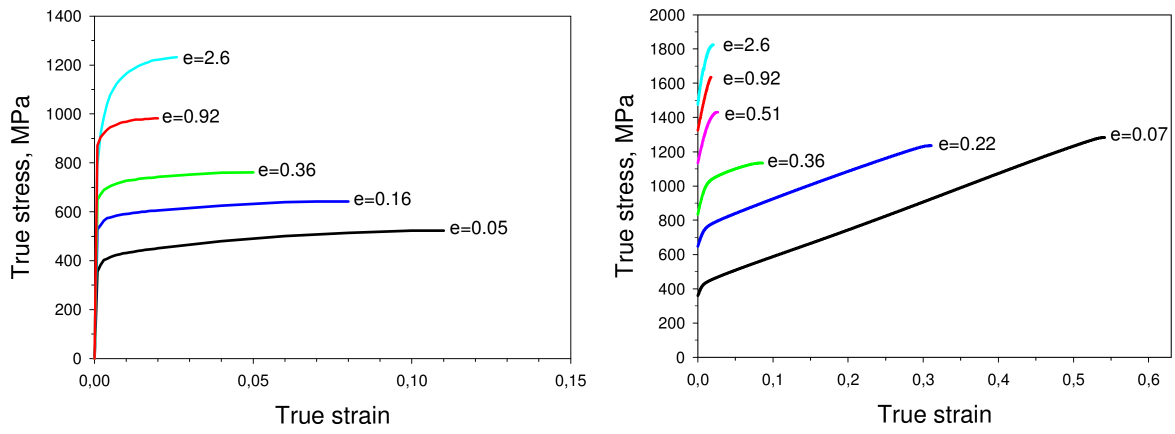

Figure 5. True stress- true strain curves for the Ti (a) and steel (b) rolled to a true thickness strain between 0.05 and 2.66. The temperature of the tension test was 293K. The true thickness strain imposed during rolling prior to tension testing is indicated in the figures.

4. Discussion

The major conditions/causes for the deformation twinning in titanium and TWIP steel are quite different: low symmetry of HCP crystalline lattice in titanium and low stacking fault energy in steel [4, 11]. That is why twin boundaries in these two types of materials have a considerable difference in their energy. Twin boundaries in TWIP steels are of type Σ3 with lowest energy and most perfect structure (high coherency). Therefore, in spite of high misorientation (60°) these boundaries are supposed to be quite transparent for moving dislocations. If so, these boundaries (i) should have a moderate or even low Hall-Petch strengthening in comparison to arbitrary high-angle grain boundaries and (ii) sluggish deviation from the coherent state in the course of interaction with lattice dislocations. These suggestions are supported by the fact that the nearly perfect twin/matrix orientation relationship survives in TWIP steels even after considerable strain [12]. Along to the propensity of dislocations for splitting (because of low SFE) all above mentioned factors result in development of a cellular microstructure which partially transforms into a grain microstructure only at strains of $\varepsilon \geq 2.66$.

The structure of twin boundaries (with misorientations corresponding to Σ7-Σ19 CSL orientation relationships) in hcp titanium is much less perfect than that of the coherent Σ3 twin boundary in fcc metals. This provides more efficient Hall-Petch strengthening. In addition, (semi)coherent twin boundaries in titanium transform during deformation into usual incoherent high-angle grain boundaries [13] yielding formation of a very fine microstructure.

Indeed, a quantitative estimation of the Hall-Petch and substructure strengthening contributions in case of Ti and TWIP steel is in good agreement with the suggestion made above. The contribution of the various strengthening mechanisms to the overall yield strength σ_y can be typically expressed as $\sigma_y = \sigma_0 + \sigma_\rho + \sigma_{H-P}$, in which σ_0 denotes the friction stress, σ_ρ is the substructure strengthening mainly due to the dislocation density and σ_{H-P} is the Hall-Petch strengthening. The Hall-Petch contribution to the flow stress is typically written in the form $\sigma_{H-P} = \dfrac{K_y}{\sqrt{d}}$. In a simplified form the substructure strengthening σ_ρ can be expressed as $\sigma_\rho = M\alpha Gb\sqrt{\rho}$, where M is the Taylor factor, α is a constant, G is the shear modulus, b is the Burgers vector, and ρ is the dislocation density.

Strengthening of titanium during cold rolling is mainly associated with the Hall-Petch effect (see details in [6]). The main contribution in strength in the steel in the current study, however, is due to the substructure strengthening. Assuming σ_0 = 120MPa, G = 72GPa, M = 3, b = 2.5×10^{-10} m, α = 0.4 and K_y = 0.011MPa×m$^{1/2}$ [14] and using data shown in figure 4, the value of Hall-Petch strengthening is approximately an order of magnitude lower than that that of substructure strengthening.

5. Summary

Microstructure evolution during plane-strain rolling of commercial-purity titanium and Fe-0.3C-23Mn-1.5Al TWIP steel at 77K was investigated. Microstructure evolution in both Ti and steel during rolling is associated with extensive twinning, following by the development of cell or subgrain structure and formation of nanograins. Less perfect structure of twin boundaries in hcp titanium provides more efficient Hall-Petch strengthening in comparison with fcc steel. Rolling to a true strain of 2.66 at 77K resulted in the formation of a microstructure with a grain size of ~80 nm or ~40 nm in Ti or steel, respectively, and ultimate tensile strength of 1100 or 1800 MPa in Ti or steel, respectively.

Acknowledgements

This work was supported by Russian Foundation for Basic Research (Grant No. 12-08-97544-p_center_a). One of the authors (DM) expresses his gratitude to the Deutsche Forschungsgemeinschaft (DFG) for financial support within the Collaborative Research Centre (SFB) 761 "Stahl ab-initio. Quantenmechanisch geführtes Design neuer Eisenbasiswerkstoffe".

References

[1] Valiev RZ, Estrin Y, Horita Z, Langdon TG, Zehetbauer MJ and Zhu YT. 2006 *JOM* **58** 33
[2] Zherebtsov SV, Salishchev GA, Galeyev RM, Valiakhmetov OR, Mironov SYu and Semiatin SL 2004 *Scripta Mater.* **51** 1147
[3] Zherebtsov SV, Dyakonov GS, Salem AA, Malysheva SP, Salishchev GA and Semiatin SL. 2011 *Mater. Sci Eng.* **A528** 3474
[4] Bouaziz O, Allain S, Scott CP, Cugy P and Barbier D. 2011 *Curr. Opin. Solid State Mater. Sci.* **15** 141
[5] Humphreys F and Hatherly M. 2004 *Recrystallization and related annealing phenomena* (Oxford: Elsevier)
[6] Zherebtsov SV, Dyakonov GS, Salem AA, Sokolenko VI, Salishchev GA and Semiatin SL 2013 *Acta Mater,* **61** 1167
[7] Moskalenko VA, Smirnov AR and Moskalenko AV. 2009 *Low Temp. Phys.* **35** 905
[8] Molodov DA, Ivanov AV and Gottstein G. 2007 *Acta Mater.* **55** 1843
[9] Molodov DA, Gorkaya T and Gottstein G. 2011 *J. Mater. Sci.* **46** 4318
[10] Cahn JW and Mishin Y. 2009 *Int. J. Mater. Res.* **100** 510
[11] Conrad H. 1981 *Prog. Mater. Sci.* **26** 123
[12] Vercammen S, Blanpain B, De Cooman BC and Wollants P. 2004 *Acta Mater.* **52** 2005
[13] Salishchev G, Mironov S, Zherebtsov S and Belyakov A. 2010 *Mater. Charact.* **61** 732
[14] Bouaziz O, Guelton N. 2001 *Mater. Sci Eng.* **A19-321** 246